

Title	Constraining the density dependence of the nuclear symmetry energy from an x-ray bursting neutron star
Author(s)	Sotani, Hajime; Iida, Kei; Oyamatsu, Kazuhiro
Citation	Physical Review C (2015), 91(1)
Issue Date	2015-01
URL	http://hdl.handle.net/2433/196043
Right	©2015 American Physical Society.
Type	Journal Article
Textversion	publisher

Constraining the density dependence of the nuclear symmetry energy from an x-ray bursting neutron star

Hajime Sotani,^{1,2,*} Kei Iida,³ and Kazuhiro Oyamatsu⁴¹*Division of Theoretical Astronomy, National Astronomical Observatory of Japan, 2-21-1 Osawa, Mitaka, Tokyo 181-8588, Japan*²*Yukawa Institute for Theoretical Physics, Kyoto University, Kyoto 606-8502, Japan*³*Department of Natural Science, Kochi University, 2-5-1 Akebono-cho, Kochi 780-8520, Japan*⁴*Department of Human Informatics, Aichi Shukutoku University, 9 Katahira, Nagakute, Aichi 480-1197, Japan*

(Received 18 September 2014; published 14 January 2015)

Neutrons stars lighter than the Sun are basically composed of nuclear matter of density up to around twice normal nuclear density. In our recent analyses, we showed that possible simultaneous observations of masses and radii of such neutron stars could constrain $\eta \equiv (K_0 L^2)^{1/3}$, a combination of the incompressibility of symmetric nuclear matter K_0 and the density derivative of the nuclear symmetry energy L that characterizes the theoretical mass-radius relation. In this paper, we focus on the mass-radius constraint of the x-ray burster 4U 1724-307 given by Suleimanov *et al.* [V. Suleimanov, J. Poutanen, M. Revnivtsev, and K. Werner, *Astrophys. J.* **742**, 122 (2011)]. We therefrom obtain the constraint that η should be larger than around 130 MeV, which in turn leads to L larger than around 110, 98, 89, and 78 MeV for $K_0 = 180, 230, 280$, and 360 MeV. Such a constraint on L is more or less consistent with that obtained from the frequencies of quasi-periodic oscillations in giant flares observed in soft gamma repeaters.

DOI: [10.1103/PhysRevC.91.015805](https://doi.org/10.1103/PhysRevC.91.015805)

PACS number(s): 04.40.Dg, 21.65.Ef

I. INTRODUCTION

Neutron stars, stellar remnants of supernova explosions at the end of massive stars, are considered to be composed of matter in extreme conditions, namely, ultrahigh density and large neutron excess. Since the temperature of the matter is generally very low compared with the typical neutron Fermi temperature, it is extremely difficult to examine the equilibrium properties of such dense cold matter in the laboratory, although highly energetic heavy-ion collisions could create hot dense matter as encountered in proton-neutron stars. Theoretically, on the other hand, the equation of state (EOS) for matter in neutron stars, hereafter referred to as neutron star matter, remains to be determined, particularly above normal nuclear density, ρ_0 . Inversely, neutron stars could be a suitable laboratory to probe the properties of cold dense matter. For example, observations of masses and radii of neutron stars would help us to constrain the EOS of neutron star matter. In fact, recent discoveries of neutron stars with about two solar mass (M_\odot) play a role in ruling out various soft EOS models [1,2]. Furthermore, estimates of radiation radii of neutron stars have been made via observations of thermonuclear x-ray bursts and thermal spectra from low-mass x-ray binaries [3–6], which could also give us a significant constraint on the EOS. Additionally, oscillation spectra radiated from a specific kind of neutron star are another observable information to see stellar properties, such as masses, radii, the EOS, rotations, and magnetic fields (e.g., [7–14]). This unique technique is known as neutron star asteroseismology. Although observational evidences for neutron star oscillations are extremely limited, quasi-periodic oscillations discovered in the afterglow of giant flare phenomena observed from soft gamma repeaters [15]

are considered to be strongly associated with oscillations of whatever portion of neutron stars. Through these observations, possible constraints on the stellar properties, particularly in the crustal region, have been discussed [16–22].

Since the details of neutron star structure obviously depend on the still uncertain EOS of neutron star matter, they have yet to be clarified. It is generally considered [23] that under a liquid metallic ocean close to the surface, neutron-rich nuclei form a Coulomb lattice in a sea of electrons and, if any, dripped neutrons. Because of the crystalline structure, the corresponding region is called a crust. As the matter density increases up to a value close to ρ_0 , it is considered that such nuclei begin to melt into uniform matter, which consists mainly of a core of the neutron star. Furthermore, non-nucleonic components such as hyperons and quarks might appear for a still higher density region inside the core, depending on the model for the neutron star matter [24]. In addition to the possibility that such non-nucleonic components appear, it is also suggested that the uncertainty from three-neutron interactions in the EOS for pure neutron matter comes into play for the same region [25]. On the other hand, neutron star matter of density below about $2\rho_0$ is relatively easier to be constrained from terrestrial nuclear experiments. This is why we will focus particularly on low-mass neutron stars that have central density ρ_c lower than $2\rho_0$. We remark that we succeeded in constructing theoretical mass and radius formulas for such low-mass neutron stars, which are written as a function of ρ_c and η , a combination of the EOS parameters that characterize the nuclear saturation properties [26].

In this paper, we systematically examine the η dependence of the mass-radius relation of low-mass neutron stars using more than 200 phenomenological EOS models [27] that are constructed in such a way as to reproduce empirical masses and radii of stable nuclei. Then, by comparing the obtained mass-radius relation with available neutron star observations,

*sotani@yukawa.kyoto-u.ac.jp

we give possible constraints on η . In particular, for this purpose, we focus on constraints on the mass-radius relation of neutron stars that were derived by Suleimanov *et al.* [28] from the observed cooling phases of the x-ray burster 4U 1724-307 located in the globular cluster Terzan 2 via different atmosphere models. This is because unlike other studies aimed at making a constraint on the mass-radius relation via the observed thermal emission from neutron stars, Suleimanov *et al.* obtained such constraints by using the whole cooling track and checking the consistency with the theoretical prediction of neutron star cooling evolution, which enables us to minimize the theoretical uncertainties in the atmosphere model during the burst phenomena [29]. As will be shown below, the resultant constraint on the density dependence of the symmetry energy is consistent with the known constraints from the quasi-periodic oscillations observed in giant flares of soft gamma repeaters [21].

II. EOS PARAMETERS

We begin with an expression for the EOS of uniform nuclear matter at zero temperature. The bulk energy per nucleon w of this matter can be generally expanded around the saturation point of symmetric nuclear matter as a function of the nucleon number density n_b and neutron excess α as [30]

$$w = w_0 + \frac{K_0}{18n_0^2}(n_b - n_0)^2 + \left[S_0 + \frac{L}{3n_0}(n_b - n_0) \right] \alpha^2, \quad (1)$$

where α is defined as $\alpha = (n_n - n_p)/n_b$ with the neutron and proton number densities n_n and n_p . That is, the case of $\alpha = 0$ corresponds to symmetric nuclear matter, while the case of $\alpha = 1$ corresponds to pure neutron matter. The parameters w_0, n_0 , and K_0 , which characterize this expansion, denote the saturation energy, saturation density, and incompressibility of symmetric nuclear matter, respectively. On the other hand, S_0 and L are the parameters associated with the symmetry energy coefficient, i.e., S_0 is the symmetry energy coefficient at $n_b = n_0$, and L is the density dependence of the symmetry energy around $n_b = n_0$. Note that among the five parameters in Eq. (1), w_0, n_0 , and S_0 can be relatively easier to constrain from empirical masses and radii of stable nuclei, while the remaining two parameters, K_0 and L , are more difficult to fix [31]. Thus, we particularly focus this paper on the parameters K_0 and L . We remark that many EOSs of nuclear matter have been proposed so far, which have various values of K_0 and L , while having reasonable values of w_0, n_0 , and S_0 (e.g., [26,31]). Although it may well be difficult to precisely describe the mass-radius relation of neutron stars by taking K_0 and L alone as free parameters, these two parameters are expected to mainly control the stiffness of the EOS of neutron-rich nuclear matter near ρ_0 and hence the structure of at least an outer part of neutron stars. In fact, we succeeded in finding a suitable combination of K_0 and L , namely, $\eta \equiv (K_0 L^2)^{1/3}$, that well characterizes the structure of low-mass neutron stars [26] in the sense that the mass-radius relation changes smoothly with η (see Fig. 3).

Now, in order to cover a wide range of η , we consider the phenomenological EOSs of neutron star matter based on the simplified version of the Thomas-Fermi method that

allows for the bulk, gradient, and Coulomb energies [31,32]. These EOS models were systematically obtained from the energy of uniform nuclear matter, which, in the limit of $n_b \rightarrow n_0$ and $\alpha \rightarrow 0$, reduces to Eq. (1) with various values of $y \equiv -K_0 S_0 / (3n_0 L)$ and K_0 . In fact, the most relevant values of w_0, n_0 , and S_0 were determined together with that of the gradient energy coefficient for given y and K_0 by fitting masses and charge radii of stable nuclei obtained from the optimal nucleon distribution to the empirical ones [33]. We remark that y corresponds to the gradient of the saturation line near $\alpha = 0$. Finally, the crustal EOS was obtained for various sets of (L, K_0) [32] by extending the Thomas-Fermi method to several shapes of nuclei in a lattice within a Wigner-Seitz approximation [33]. Hereafter, the resultant EOSs are referred to as the OI-EOSs.

The OI-EOSs adopted here have a range of $y < -200 \text{ MeV fm}^3$ and $180 \leq K_0 \leq 360 \text{ MeV}$, which results in the range of L as $0 < L < 180 \text{ MeV}$. Note that not only does such a parameter range equally well reproduce empirical mass and radius data for stable nuclei, but also effectively covers even extreme cases [31]. We also remark that according to comprehensive reanalysis of recent data on the giant monopole resonance energies, K_0 should be in the range of $250 < K_0 < 315 \text{ MeV}$ [34], while the generally accepted value of K_0 is in the range of $K_0 = 230 \pm 40 \text{ MeV}$ [35]. That is, systematic errors in experimentally determining K_0 are still likely to be large. It is thus reasonable that the OI-EOSs used here have 247 sets of (y, K_0) , i.e., the combination of 13 different values of y ($y = -200, -220, -250, -300, -350, -400, -500, -600, -800, -1000, -1200, -1400$, and -1800 MeV fm^3) and 19 different values of K_0 ($K_0 = 180, 190, 200, \dots, 360 \text{ MeV}$). For these OI-EOSs, the corresponding values of η are calculated, which are shown in Fig. 1 as a function of L . From this figure, one can observe that the dependence of η on L is much stronger than that on K_0 . This is partly because uncertainties in L are relatively large compared with those of K_0 and partly because the power of L in η is larger than that of K_0 .

Additionally, for comparison, we show S_0 and L for the 247 OI-EOSs in Fig. 2. A strong correlation between S_0 and L was pointed out in [31] and is consistent with the values

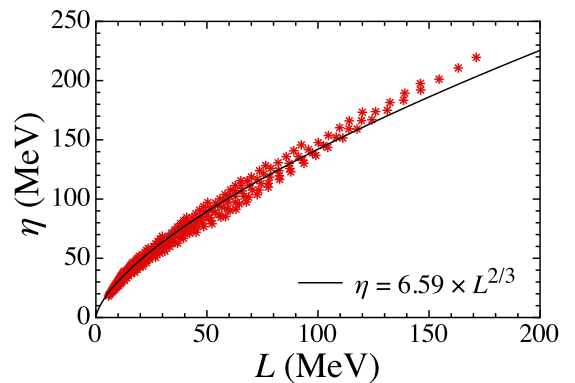


FIG. 1. (Color online) η as a function of L . The dots are taken from the 247 OI-EOSs, while the solid line denotes the fitting in a functional form of $L^{2/3}$.

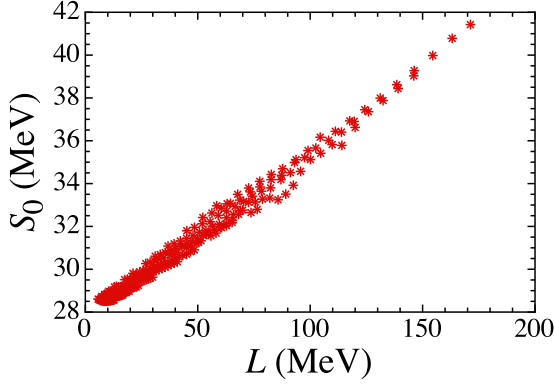


FIG. 2. (Color online) Parameter S_0 plotted as a function of L for the 247 OI-EOSs.

of S_0 and L obtained via fitting to experimental data on nuclear masses and radii on the 1σ level with the nuclear energy density functional for Skyrme type interaction [36]. As compared with this correlation, the correlation between η and L is equally strong. Via simultaneous observations of masses and radii of low-mass neutron stars, therefore, constraints on η and thus L would be available to some extent. Finally, in Fig. 1, we also show the fitting to the data of the 247 OI-EOSs, i.e., $\eta = 6.59(\frac{L}{1 \text{ MeV}})^{2/3}$ MeV, which corresponds to $K_0 = 286.8$ MeV.

III. CONSTRAINTS ON η AND L

Following the finding of η , we here give a possible constraint on η from observations of masses and radii of low-mass neutron stars. Unfortunately, however, no firm observational evidence for the presence of less-than- $1M_\odot$ neutron stars is available. Even more challenging is simultaneous mass and radius determination of low-mass neutron stars. Thermonuclear x-ray bursts in low-mass x-ray binaries help to determine the masses and radii of the bursting neutron stars, although there exist many uncertainties both in theoretical models and in observations. In fact, it is not straightforward to determine the exact moment when the luminosity reaches the Eddington limit at the star's surface, if data for the photospheric radius expansion bursts are adopted to determine the star's mass and radius. Additionally, the color-correction factor defined as the ratio of the color temperature to the effective temperature of the source object is sensitive to the flux during the cooling tail as well as the model of neutron star atmospheres [29]. To minimize uncertainties in the theoretical models that determine the Eddington luminosities during the burst phenomena, Suleimanov *et al.* suggested using information from the whole cooling track in the x-ray bursts, and succeeded in obtaining the constraint on the mass and radius of the x-ray burster 4U 1724-307 located in the globular cluster Terzan 2 by using various atmosphere models [28]. In this paper, we adopt their results, which imply a relatively low-mass neutron star, to obtain a constraint on η and L .

In particular, Suleimanov *et al.* adopted three atmosphere models with different chemical compositions, i.e., pure hydrogen, pure helium, and the solar H/He composition with

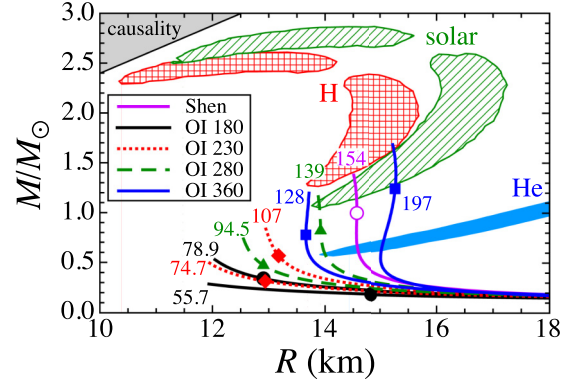


FIG. 3. (Color online) Allowed regions in the mass-radius relation obtained from the observation of the x-ray burster 4U 1724-307 by Suleimanov *et al.* [28], where they adopted three different atmosphere models, i.e., pure hydrogen (checkered region), pure helium (filled region), and the solar ratio of H/He with subsolar metal abundance $Z = 0.3Z_\odot$ (shaded region). On the other hand, the lines with marks denote the stellar models constructed from nine EOSs with different values of η (attached numbers) for $\rho_c \leq 2.0\rho_0$, where each mark corresponds to the mass and radius of a star with $\rho_c = 1.5\rho_0$. Additionally, the upper left region is ruled out by the causality [38].

subsolar metal abundance $Z = 0.3Z_\odot$ appropriate for Terzan 2 [37]. Then, assuming a flat distribution of the distance from the Earth between 5.3 and 7.7 kpc with Gaussian tails of $1\sigma = 0.6$ kpc, they obtained such constraints in the mass-radius relation within 90% confidence level as shown in Fig. 3, where the checkered, filled, and shaded regions correspond to the constants obtained with the atmosphere models composed of pure hydrogen, pure helium, and the solar H/He with $Z = 0.3Z_\odot$, respectively. In addition to their results, we show the region ruled out by the causality, which is given by $R < 2.824GM/c^2$ [38]. From this figure, one can observe that the radius of the x-ray burster 4U 1724-307 should be relatively large if the star's mass has a canonical value of order $1.4M_\odot$.

In Fig. 3, we also plot the stellar models constructed with several sets of the OI-EOSs and the Shen EOS [39], where the corresponding value of η is written on each EOS. Here, we particularly focus on the stellar models for $\rho_c \leq 2.0\rho_0$ to avoid uncertainties in the EOS at high density due to the possible appearance of non-nucleonic components and/or the profoundness of three-neutron interactions as mentioned above. In Fig. 3, therefore, the upper end of each line corresponds to the stellar model constructed with $\rho_c = 2.0\rho_0$; for reference, we also show the stellar model for $\rho_c = 1.5\rho_0$ by putting a mark on each line.

Now, assuming that the x-ray burster 4U 1724-307 has a canonical neutron star mass and that the EOS is universal in the sense that all neutron stars can be constructed with a single EOS, one can conclude from Fig. 3 that η is larger than ~ 130 MeV. Via $L = \sqrt{\eta^3/K_0}$, $\eta \gtrsim 130$ MeV leads to $L \gtrsim 110$ MeV for $K_0 = 180$ MeV, $L \gtrsim 98$ MeV for $K_0 = 230$ MeV, $L \gtrsim 89$ MeV for $K_0 = 280$ MeV, and $L \gtrsim 78$ MeV for $K_0 = 360$ MeV. One can more clearly see the allowed

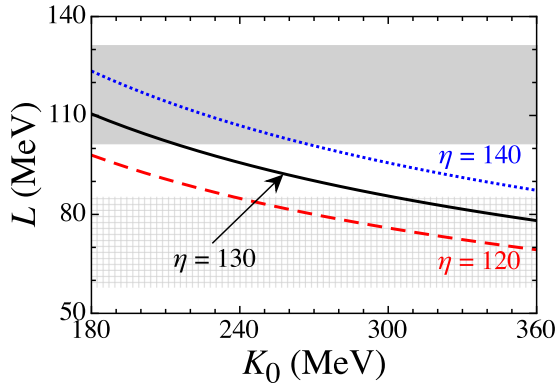


FIG. 4. (Color online) Nuclear matter EOS parameters constrained from $\eta \geq 130$ MeV, which correspond to the region above the solid line. For reference, $\eta = 120$ and 140 MeV are plotted with the dashed and dotted lines. We also display the parameter space constrained from the observations of quasi-periodic oscillations in giant flares with the filled and checkered regions [21] (see text for details).

region in the parameter space in Fig. 4, i.e., the region above the solid line, where we show the lines for $\eta = 120$ MeV (dashed line) and 140 MeV (dotted line) for reference. We remark that the density at the core-crust boundary strongly depends on the value of L [32], which is a crucial property to determine the crust mass and moment of inertia. Combining Fig. 5 in Ref. [32] with the constraint on L obtained here from the neutron star observations, the nucleon number density at the crust basis is expected to be around 0.07 fm^{-3} .

Recently, a lower limit of observed neutron star radii has been additionally suggested from another object. That is, the neutron star radius in the low-mass x-ray binary 4U 1608-52 is predicted from the hard-state burst occurring during the low-accretion rate to be larger than 13 km , if the neutron star mass is in the range of $1.2M_{\odot}$ – $2.4M_{\odot}$ [40]. This suggestion also indicates a large value of η , i.e., $\eta \gtrsim 100 \text{ MeV}$, which covers the constraint obtained from the x-ray burster 4U 1724-307. Thus, η is predicted to be larger than around 130 MeV from both of the astronomical observations.

We conclude this section by noting that observations of neutron star oscillations could also tell us the properties of neutron star matter. In fact, the gravitational waves emitted from oscillating neutron stars could provide a possible way to see the neutron star properties, although they have not yet been observed directly. Another possibility is the detection of electromagnetic waves associated with neutron star oscillations [41,42]. Fortunately, quasi-periodic oscillations have been discovered in the afterglow of giant flares observed from soft gamma repeaters [15]. If such oscillations result

from crustal torsional oscillations, a fairly strong constraint on L can be obtained by comparing the observed frequencies of quasi-periodic oscillations with theoretical predictions of the eigenfrequencies of the torsional modes [19–21]. In this way, we obtained two possible constraints on L . One is $101.1 \leq L \leq 131.0 \text{ MeV}$, which explains all the observed frequencies lower than 100 Hz in terms of the crustal torsional oscillations, while the other is $58.0 \leq L \leq 85.3 \text{ MeV}$ if the second lowest frequency observed in SGR 1806-20 would be excited by a different mechanism from the crustal oscillations. These constraints on L are also shown in Fig. 4 by the filled region for the former constraint and by the checkered region for the latter one. As can be seen from this figure, the former constraint on L is more consistent with the constraint from $\eta \gtrsim 130 \text{ MeV}$ than the latter one. On the other hand, we remark that most of the terrestrial nuclear experiments suggest somewhat lower values of L [43], although there still exists large uncertainty in L [44]. We also remark that the EOS of pure neutron matter calculated within the chiral effective field theory favors smaller values of L (see [45] and references therein). Anyway, η (and L) could be significantly smaller than our constraint, if constraints on M and R of several neutron stars (e.g., [3–6]), other than the ones adopted in the present analysis, are taken for granted.

IV. CONCLUSION

We apply the classification of the EOS of neutron star matter in terms of η as developed in Ref. [26] to the mass-radius relation constrained from observations of the x-ray burster 4U 1724-307 and remark on a possible constraint on η , which gives important information on the density dependence of the symmetry energy. In order to obtain a better constraint on η , it would be significant to expect simultaneous mass and radius determination of low-mass neutron stars from the neutron star interior composition explorer (NICER) by NASA and/or the large observatory for x-ray timing (LOFT) by ESA via observations of pulse profiles from hot rotating neutron stars [46].

ACKNOWLEDGMENTS

H.S. is grateful to V. Suleimanov and J. Poutanen for providing us with their data in preparing Fig. 3. This work was supported in part by Grants-in-Aid for Scientific Research on Innovative Areas through No. 24105001 and No. 24105008 provided by MEXT, by Grant-in-Aid for Young Scientists (B) through No. 26800133 provided by JSPS, by the Yukawa International Program for Quark-Hadron Sciences, and by the Grant-in-Aid for the global COE program “The Next Generation of Physics, Spun from Universality and Emergence” from MEXT.

- [1] P. B. Demorest, T. Pennucci, S. M. Ransom, M. S. E. Roberts, and J. W. T. Hessels, *Nature* **467**, 1081 (2010).
- [2] J. Antoniadis *et al.*, *Science* **340**, 1233232 (2013).

- [3] F. Özel, G. Baym, and T. Güver, *Phys. Rev. D* **82**, 101301 (2010).
- [4] A. W. Steiner, J. M. Lattimer, and E. F. Brown, *Astrophys. J.* **765**, L5 (2013).

- [5] S. Guillot, M. Servillat, N. A. Webb, and R. E. Rutledge, *Astrophys. J.* **772**, 7 (2013).
- [6] J. M. Lattimer and A. W. Steiner, *Astrophys. J.* **784**, 123 (2014).
- [7] N. Andersson and K. D. Kokkotas, *Phys. Rev. Lett.* **77**, 4134 (1996).
- [8] N. Andersson and K. D. Kokkotas, *Mon. Not. R. Astron. Soc.* **299**, 1059 (1998).
- [9] H. Sotani, K. Tominaga, and K. I. Maeda, *Phys. Rev. D* **65**, 024010 (2001).
- [10] H. Sotani and T. Harada, *Phys. Rev. D* **68**, 024019 (2003).
- [11] H. Sotani, K. Kohri, and T. Harada, *Phys. Rev. D* **69**, 084008 (2004).
- [12] A. Passamonti and N. Andersson, *Mon. Not. R. Astron. Soc.* **419**, 638 (2012).
- [13] H. Sotani, N. Yasutake, T. Maruyama, and T. Tatsumi, *Phys. Rev. D* **83**, 024014 (2011).
- [14] D. D. Doneva, E. Gaertig, K. D. Kokkotas, and C. Krüger, *Phys. Rev. D* **88**, 044052 (2013).
- [15] A. L. Watts and T. E. Strohmayer, *Adv. Space Res.* **40**, 1446 (2006).
- [16] A. W. Steiner and A. L. Watts, *Phys. Rev. Lett.* **103**, 181101 (2009).
- [17] M. Gearheart, W. G. Newton, J. Hooker, and B. A. Li, *Mon. Not. R. Astron. Soc.* **418**, 2343 (2011).
- [18] H. Sotani, *Mon. Not. R. Astron. Soc.* **417**, L70 (2011).
- [19] H. Sotani, K. Nakazato, K. Iida, and K. Oyamatsu, *Phys. Rev. Lett.* **108**, 201101 (2012).
- [20] H. Sotani, K. Nakazato, K. Iida, and K. Oyamatsu, *Mon. Not. R. Astron. Soc.* **428**, L21 (2013).
- [21] H. Sotani, K. Nakazato, K. Iida, and K. Oyamatsu, *Mon. Not. R. Astron. Soc.* **434**, 2060 (2013).
- [22] H. Sotani, *Phys. Lett. B* **730**, 166 (2014).
- [23] J. M. Lattimer and M. Prakash, *Science* **304**, 536 (2004).
- [24] P. Haensel, A. Y. Potekhin, and D. G. Yakovlev, in *Neutron Stars 1: Equation of State and Structure* (Springer, Berlin, 2006).
- [25] S. Gandolfi, J. Carlson, and S. Reddy, *Phys. Rev. C* **85**, 032801 (2012).
- [26] H. Sotani, K. Iida, K. Oyamatsu, and A. Ohnishi, *Prog. Theor. Exp. Phys.* **2014**, 051E01 (2014).
- [27] K. Iida and K. Oyamatsu, *Eur. Phys. J. A* **50**, 42 (2014).
- [28] V. Suleimanov, J. Poutanen, M. Revnivtsev, and K. Werner, *Astrophys. J.* **742**, 122 (2011).
- [29] V. Suleimanov, J. Poutanen, and K. Werner, *Astron. Astrophys.* **527**, A139 (2011).
- [30] J. M. Lattimer, *Annu. Rev. Nucl. Part. Sci.* **31**, 337 (1981).
- [31] K. Oyamatsu and K. Iida, *Prog. Theor. Phys.* **109**, 631 (2003).
- [32] K. Oyamatsu and K. Iida, *Phys. Rev. C* **75**, 015801 (2007).
- [33] K. Oyamatsu, *Nucl. Phys. A* **561**, 431 (1993).
- [34] J. R. Stone, N. J. Stone, and S. A. Moszkowski, *Phys. Rev. C* **89**, 044316 (2014).
- [35] E. Khan and J. Margueron, *Phys. Rev. C* **88**, 034319 (2013).
- [36] M. Kortelainen, T. Lesinski, J. Moré, W. Nazarewicz, J. Sarich, N. Schunck, M. V. Stoitsov, and S. Wild, *Phys. Rev. C* **82**, 024313 (2010).
- [37] S. Ortolani, E. Bica, and B. Barbuy, *Astron. Astrophys.* **326**, 614 (1997).
- [38] J. M. Lattimer, *Annu. Rev. Nucl. Part. Sci.* **62**, 485 (2012).
- [39] H. Shen, H. Toki, K. Oyamatsu, and K. Sumiyoshi, *Nucl. Phys. A* **637**, 435 (1998).
- [40] J. Poutanen, J. Nättälä, J. J. E. Kajava, O.-M. Latvala, D. K. Galloway, E. Kuulkers, and V. F. Suleimanov, *Mon. Not. R. Astron. Soc.* **442**, 3777 (2014).
- [41] H. Sotani, K. D. Kokkotas, P. Laguna, and C. F. Sopuerta, *Phys. Rev. D* **87**, 084018 (2013).
- [42] H. Sotani, K. D. Kokkotas, P. Laguna, and C. F. Sopuerta, *Gen. Relativ. Gravit.* **46**, 1675 (2014).
- [43] M. B. Tsang *et al.*, *Phys. Rev. C* **86**, 015803 (2012).
- [44] W. G. Newton, M. Gearheart, D. H. Wen, and B. A. Li, *J. Phys.: Conf. Ser.* **420**, 012145 (2013).
- [45] K. Hebeler and A. Schwenk, *Eur. Phys. J. A* **50**, 11 (2014).
- [46] D. Psaltis, F. Özel, and D. Chakrabarty, *Astrophys. J.* **787**, 136 (2014).